

Determining Hydraulic Conductivity from Soil Characteristics with Applications for Modelling Stream Discharge in Forest Catchments

Marie-France Jutras and Paul A. Arp
*Faculty of Forestry and Environmental Management
University of New Brunswick
Fredericton, NB
Canada*

1. Introduction

Many applications in watershed management, forestry, agriculture, and horticulture require hydrologically feasible estimates for assessing the rate at which water infiltrates and percolates through the soil, and how much of that is either taken up by the vegetation or passes through the ground until entering flow channels and streams further below in the landscape. In the literature, there are many approaches to do this, ranging from direct field measurements to numerical and theoretical constructs (Di Frederico and Tartakosky 2000; Pachepsky and Rawls 2005; Sudicky et al. 2010). Field measurements focus on, e.g., (i) direct measurements regarding the rate of infiltration, (ii) hydraulic gradients and hydraulic conductivities along hillslopes and aquifers, and (iii) stream discharge. Theoretical means infer soil and subsoil water retention and hydraulic conductivities from basic soil properties such as soil texture, organic matter content, and density. In turn, these estimates can then be used to determine temporal changes in soil moisture and soil moisture flow within fields (or hydrological response units), along hill slopes and across catchments, by way of simple trickle-down models (e.g., Church 1997), or complex geographically distributed hydrology models (Kim et al. 2008). The most elaborate models generate atmosphere-vegetation-soil transference fluxes based on empirical Eddy correlation techniques (Kuchment et al. 2006), while the simpler models use weather records involving precipitation and air temperature to assess daily changes in soil moisture and water flow (Balland et al. 2006; Murphy et al. 2009). This chapter (i) presents a generalized framework for estimating soil hydraulic conductivities at saturation, i.e., K_{sat} , at the soil-layer level, and (ii) applies this framework for modelling water retention and stream discharge for six well-studied forest catchments across Canada, from east to west. Within this framework, special attention is given to ensure that

- i. soil moisture content at field capacity (FC) is always smaller than soil moisture content at the saturation point (SP),
- ii. the permanent wilting point (PWP) is always smaller than FC,

- iii. the bulk density of the soil (D_b) is always smaller than the mean particle density (D_p) of the soil,
- iv. K_{sat} is strongly affected by the pore space of the soil, and
- v. estimates for D_b , D_p , SP , FC , PWP and K_{sat} are functionally related to soil depth, texture, and organic matter content (OM) across a wide range of natural soil conditions, from organic to mineral, from loose to compact, and from shallow to deep.

2. Estimating soil moisture flow, retention, and K_{sat}

Equations that generate layer-specific estimates for D_b , D_p , FC , PWP and K_{sat} from generally available soil data such as OM , texture (i.e., sand, silt and clay content) and soil depth are known as “point pedotransfer functions”, or point PTFs (Bouma, 1989; Gijssman et al. 2003; Børgesen and Schaap 2005; Pachepsky and Rawls 2005; Schaap 2006; Børgesen et al. 2007). The following equations (Balland et al. 2008) were used to this effect:

$$D_b = \frac{a_{D_b} + (D_p - a_{D_b} - b_{D_b} \text{ SAND}) [1 - \exp(-c_{D_b} \text{ DEPTH})]}{1 + d_{D_b} \text{ OM}} \quad (1)$$

$$FC = SP \left(1 - \exp \left(\frac{-a_{FC} (1 - \text{SAND}) - b_{FC} \text{ OM}}{SP} \right) \right) \quad (2)$$

$$PWP = FC \left(1 - \exp \left(\frac{-a_{PWP} \text{ CLAY} - b_{PWP} \text{ OM}}{FC} \right) \right) \quad (3)$$

$$\log_{10} K_{sat} = a_{K_{sat}} + b_{K_{sat}} \log_{10}(D_p - D_b) + c_{K_{sat}} \text{ SAND} \quad (4)$$

where a , b , c , and d are D_b -, FC -, PWP - and K_{sat} -specific calibration coefficients, and

$$\frac{1}{D_p} = \frac{OM}{D_{p_{OM}}} + \frac{1 - OM}{D_{p_{min}}} \quad (5)$$

determines the average value for D_p , with $D_{p_{OM}} = 1.3 \text{ gcm}^{-3}$ and $D_{p_{min}} = 2.65 \text{ gcm}^{-3}$ referring to the particle density of soil organic matter and minerals, respectively. SAND , CLAY , OM , FC , PWP , and FC refer to f dry soil weight fractions (fine earth fraction only). DEPTH refers to the mid depth of each soil layer, in cm. K_{sat} is expressed in cm hr^{-1} . Calibrating these equations with data taken from New Brunswick (NB) and Nova Scotia (NS) soil survey reports (CANSIS, 2000) produced the following results:

$$D_b = \frac{1.23 + (D_p - 1.23 - 0.75 \text{ SAND}) (1 - \exp(-0.0106 \text{ DEPTH}))}{1 + 6.83 \text{ OM}} \quad (6)$$

$$FC = SP \left(1 - \exp \left(\frac{-0.588 (1 - \text{SAND}) - 1.73 \text{ OM}}{SP} \right) \right) \quad (7)$$

$$PWP = FC \left(1 - \exp \left(\frac{-0.511 \text{ CLAY} - 0.865 \text{ OM}}{FC} \right) \right) \quad (8)$$

$$\log_{10}K_{sat} = -0.98 + 7.94 \log_{10}(D_p - D_b) + 1.96 \text{ SAND} \quad (9)$$

with the best-fitted values for R², MAE, RMSE and the corresponding a, b, c and d regression coefficients listed in Table 1. These results show that the precision so achieved varied in the following order: FC > PWP > Db > Ksat. This order likely reflects the extent by which changes in soil structure (or state of soil aggregation) affect the measurement of these variables. It appears that such changes have (i) only small if any effects on the pressure-plate determinations for FC and PWP, (ii) moderate effects on the in-situ Db determinations, but (iii) large effects on Ksat on account of disproportionate flow rates through fine to large pores, root channels and cracks. With organic soils, varying degrees of humification also matter, with well-humified matter being more compactable and less permeable than fibrous matter (Pepin et al., 1992; Paquet et al., 1993; Balland et al. 2008). The modelled variations of Ksat with changing OM, sand content, and Db are shown in Figure 1, together with plots of actual versus best-fitted NB and NS data.

Property	ax	bx	cx	dx	R ²	MAE	RMSE
Db, g cm ⁻³	1.17 ±0.05	0.83 ±0.08	0.022 ±0.004	6.1 ±0.8	0.83	0.14	0.18
FC, g g ⁻¹	0.588 ±0.016	1.734 ±0.049			0.96	0.032	0.048
PWP, g g ⁻¹	0.511 ±0.025	0.865 ±0.057			0.65	0.026	0.035
log ₁₀ Ksat	-0.98 ±0.11	7.94 ± 0.48	1.96 ±0.21		0.80	0.38	0.49

Subscript x for a, b, c d mean Db, FC, PWP, or Ksat, as pertinent by row

Table 1. Best-fitted results for Db, FC, PWP, and Ksat (cm hr⁻¹) including their respective a, b, c, and d coefficients, coefficient of determination (R²), mean absolute error (MAE) and root mean square error (RMSE) for the New Brunswick and Nova Scotia soils data, based on Eqs. 1 to 4.

The extent of inter-parametric correlations among the regression coefficients is shown in Table 2. These correlations should, ideally, be as close to zero as possible to narrow the equifinal solution space for the best-fitted a, b, c and d coefficients. For example, the -0.89 correlation between a_{Ksat} and c_{Ksat} implies that an increase in c_{Ksat} will produce a corresponding decrease in a_{Ksat}. Hence, large non-zero inter-coefficient correlations numbers imply large uncertainties about the best-fitted coefficients for the parameter pair so identified.

Applying the Ksat formulation to the Universal Soil Database (UNSODA, Leij 1996), instead of NB and NS data yielded,

$$\log_{10}K_{sat} = (-1.05 \pm 0.08) + (6.1 \pm 0.4) \log_{10}(D_p - D_b) + (2.2 \pm 0.1) \text{ SAND} \quad (10)$$

$$(n = 481; R^2 = 0.52; RMSE = 0.68; MAE = 0.54).$$

Db	a _x	b _x	c _x	d _x	log ₁₀ Ksat	a _x	b _x	c _x
a _x	1				a _x	1		
b _x	-0.0067	1			b _x	-0.043	1	
c _x	-0.45	-0.75	1		c _x	-0.89	-0.15	1
d _x	0.77	0.062	-0.16	1				
FC	a _x	b _x			PWP	a _x	b _x	
a _x	1				a _x	1		
b _x	-58	1			b _x	-0.34	1	

Table 2. Correlation coefficients between a, b, c and d parameters of equations 1 to 4, New Brunswick and Nova Scotia soil data.

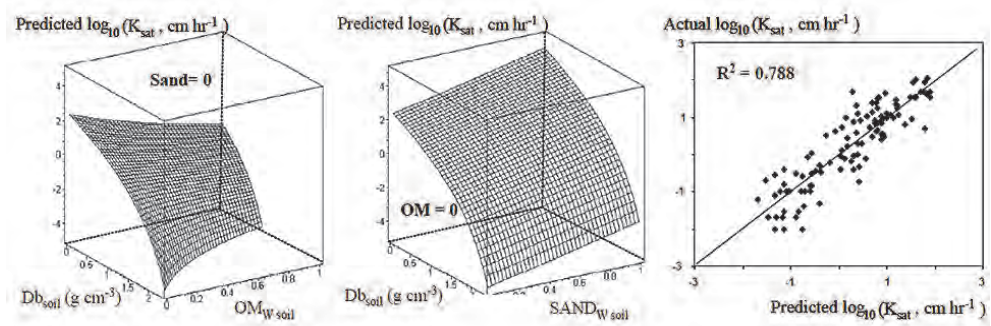


Fig. 1. Left and middle: 3-D visualisations of how $\log_{10}K_{sat}$ varies with increasing soil bulk density (Db), sand fraction and organic matter (OM) fraction. Right: best-fitted $\log_{10}K_{sat}$ versus actual data (right).

Hence, the $\log_{10}K_{sat}$ formulation based on the NS and NB data alone remained valid in its general form, but the coefficient values changed slightly, with the largest change associated with the $\log_{10}(D_p - Db)$ coefficient, i.e., dropping from 7.9 to 6.1. This change may relate to procedural differences, e.g., using estimated D_p values from known SP and Db values (NB and NS data) versus direct D_p measurements (UNSODA). The plot of actual versus best-fitted values in Figure 2 suggests a general agreement between the above K_{sat} formulation and the data from both sources.

3. Catchment hydrology

The Forest Hydrology Model (ForHyM; Balland et al. 2006; Fig 3) was used to simulate the hydrothermal conditions within each of the discharge-monitored basins listed in Table 3. These simulations were driven by local weather records for daily precipitation (rain, snow) and air temperature. In this model, only gravitational water was allowed to flow, i.e., the amount of soil moisture above FC. The rate of this flow was set to be proportional to pore % of gravitational water multiplied by K_{sat} to estimate downward flow ("percolation", or "infiltration"), and adjusted for % slope of the

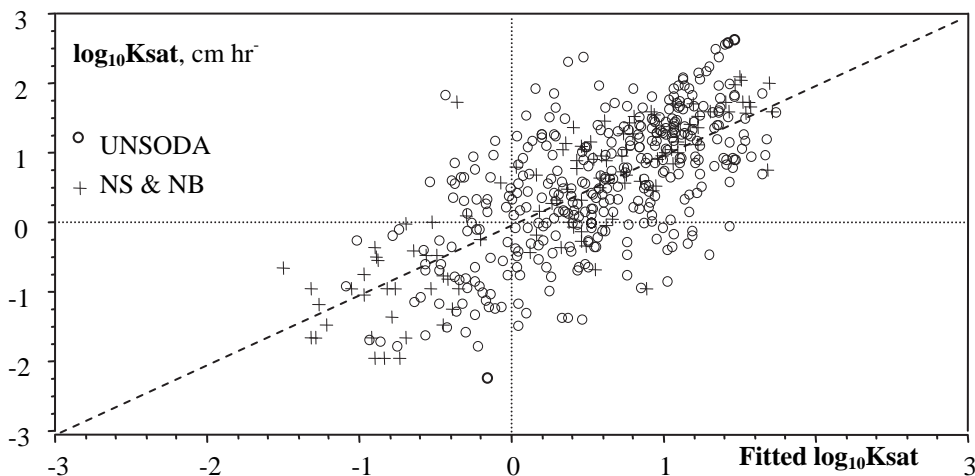


Fig. 2. Scatter plot of actual versus best-fitted Ksat values (Eq. 10) for two data sources (UNSODA (Leij et al. 1996; NB & NS soil survey data, Balland et al. 2008).

basin to estimate “lateral flow” or “interflow”. At saturation, downward flow into the next mineral soil was typically slower than lateral flow on account of decreasing Ksat with increasing soil density at lower soil depth. Infiltration into unsaturated soils was determined (i) by directly filling the partially available pore space up to SP, and (ii) by accommodating downward as well as lateral flow as long as the soil moisture content would remain above FC. For simplicity, the soil at each location was represented by the forest floor (or LFH layer), the A and B layers combined, and the C layer. The substrate below the C layer was represented by 1 m intervals to a depth of 12 m, i.e., to the depth of isothermal conditions year-round. Values for D_p , D_b , SP, FC, PWP, Ksat were generated for each layer from local soil surveys, using Eqs. 1 to 9 (Table 4). Estimates for the moisture- and frost-varying heat capacity and conductivity were also generated for each layer according to Balland and Arp (2005). The outcomes of these calculations are illustrated in Figure 4 for a basin at Turkey Lakes in Ontario near Sault St. Marie north of Lake Superior, and the Moosepit Brook basin east of Kejimikujik National Park, Nova Scotia. The general conformance between the modelled and actual stream discharge is documented in Table 5 by way of the best-fitted regression coefficient and the corresponding R^2 and RMSE values for each of the basins examined. The Ksat multiplier adjustments for the downward and lateral flow components are entered in Table 4. No adjustments were made to the layer-estimated values for D_b , D_p , FC, and PWP (Eqs. 5 to 8). The following can be observed from Figs. 4 and 5 and Tables 1 to 5:

- i. There is generally good agreement between the actual and basin calibrated snowpack depth, and stream discharge at the daily to annual time scales (Fig. 4, Table 5).
- ii. No adjustments were needed to match the monitored stream discharge with the incoming precipitation and model-assessed evapotranspiration rates.

- iii. The Ksat adjustments for downward flow varied from 0.5 to 2 (Table 4), and were therefore within the generically determined precision for Ksat based on Eqs. 9 and 10 and the layer specification for soil texture, organic matter, soil depth and soil density (Table 1).
- iv. The Ksat adjustments for lateral flow were more variable, thereby indicating that lateral flows through the basins were more complex and generally low thereby requiring downward Ksat adjustments for interflow, especially for the hummocky basins (Table 4). This was likely due to flow obstructions such as mounds and pits, empty or partially filled water pools above and below the regolith, erratic changes in soil depth, density, texture, organic matter, coarse fragment, and variations in the surface exposure of partially fractured bedrock especially along ridges, steep slopes and within crevices. Hayward Brook was particularly exceptional with its < Ksat multipliers for lateral flow. This undulating to rolling basin is underlain by calcareous shales, which generally have high flow variabilities, thereby enhancing downward flow (Schulze-Makuch et al. 1999).
- v. For most soils, Db generally increases with soil depth (Eq. 1), and Ksat decreases accordingly (Eqs. 9 and 10). Within the A and B layers, Ksat values range from about 50 to 500 cm hr⁻¹. Within the subsoil, Ksat values are generally much lower by one to two orders of magnitude, especially on compacted tills.
- vi. The Ksat value for the forest floor, as projected by way of Eq. 5, is rather low, but corresponds to Ksat values normally associated with organic soils. Due to the high porosity of this layer, infiltration occurs quickly. The water so received is, however, released rather slowly to the underlying forest soil and only so once the field capacity of the forest floor is exceeded. As a result, soil layers underneath the forest floor often remain quite dry during the later portion of the summer and during early fall. At this time, soils may also become hydrophobic. As a result, surface water would then flow laterally over short distances towards nearby pits and depressions, where the soil would be moister and permit gradual infiltration and downward percolation.
- vii. The calibrated Ksat values for and depression lateral and downward flow generally fall within the Ksat uncertainty range associated with Eq. 9 and Eq. 10, with the best-fitted RSME values for Ksat varying from about ±0.4 to ±0.6. This range is similar to that obtained with (i) testing water recharge in wells receiving water from small depressions (about 50 m²) to catchments up to about 1200 ha or more, and after taking care of the scaling-up effect that is associated with these measurements ($\log_{10}K_{sat}$ RMSE = ±0.61; Schulze-Makuch et al. 1999), and (ii) using tension infiltrometers and Guelph permeameters to determine Ksat by soil depth at Turkey Lakes ($\log_{10}K_{sat}$, RMSE = ± 0.45; Murray and Buttle 2006) and at Lac Laflamme, as detailed in Table 4.
- viii. Since the study locations represent a range of catchment size from about 70 to 1700 ha, there are no obvious trends with catchment size. Hence, the model-derived Ksat adjustments for the LFH, A&B and C layers are essentially independent of scale across this range. This is also in general agreement with Schulze-Makuch et al. (1999) who found that the up-scaling requirement for Ksat generally stops once the Ksat-determining flow fields offer no additional heterogeneity. However, Laudon et al. (2007) concluded that stream discharge is less dependent on scale than on wetland

coverage per catchment, with discharge contributions of “event” water (or new water) amounting to 50% in wetland dominated catchment while limited to 10% to 30% in forest dominated catchments. Considering also

- a. that forest catchments are generally permeated by many converging flow channels with varying and weather-dependent thresholds for flow initiation,
- b. that forest catchments in glaciated landscapes such as the ones of this study are generally underlain by a layer of surface-fractured bedrock, and
- c. that this layer provides additional space for water pooling and hydraulically activated flows towards the streams,

it is reasonable to suggest that the K_{sat} estimates and their multipliers in Tables 3 and 4 reflect similar flow heterogeneities within each of the many subcatchments for the catchments of this study.

- ix. The above approach requires layer-specific estimates for K_{sat} . If these are not available, then K_{sat} can be derived from layer-representative values for sand content, D_p and D_b . When estimates for D_p and D_b are not available, one can derive these via Eqs. 5 and 6 for any soil depth and given values for sand and organic content. Generally, these values need to be representative of the LHF, A, B and C layers. The sensitivity of the resulting K_{sat} estimates to the natural variations of these quantities can be evaluated via Eq.s. 5, 6, and 9 or 10.

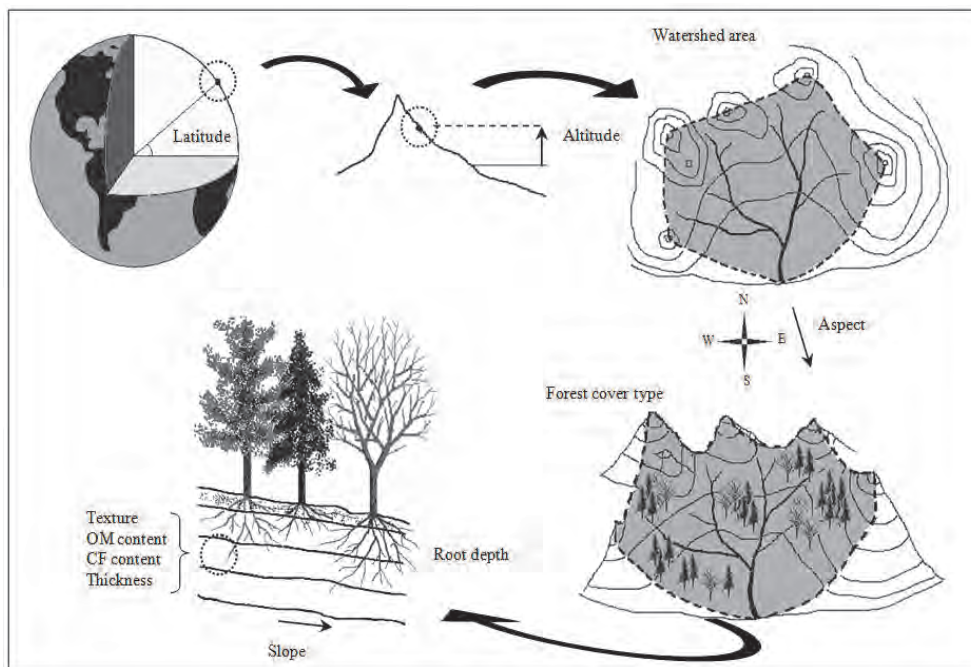


Fig. 3. Specification overview for the Forest Hydrology Model ForHyM (Balland 2002).

Site Parameters	Moosepit Brook Nova Scotia (NS)	Peggy Brook Nova Scotia (NS)	Hayward Brook New Brunswick (NB)	Turkey Lakes Ontario (ON)	Lac Laflamme Quebec (QB)	Ribbet River Vancouver Island, British Columbia (BC)
References	Bobba et al. 1986 Juras et al. 2011	Juras et al. 2011	Chi 2008	Murphy et al. 2009; Beall et al. 2001 Murray and Bault 2005	Barry et al. 1987; 1990 Stein et al. 1994	Zhu & Mazumder 2008
Abbreviation	MP	PB	HB	TL	LL	GB
Latitude (N)	44°28'	44°49'	45°52'	47°03'	47°17'	48°32'
Longitude (W)	65°03'	63°51'	65°11'	84°25'	71°14'	123°42'
Area (ha)	1670	196	508	1050	69	1630
Elevation (m)	100-150	172-227	96-162	350-400	777-884	375
Slope (%)	1	7	8	8	11	17
Deciduous:coniferous	50:50	75:25	50:50	100:0	10:90	0:100
Rooting habit	Medium	Shallow	Medium	Deep	Medium	Deep
Forest floor depth (cm)	5	5	5	7	8	15
Mineral soil: depth (cm); texture	42: SL	70: SL	40: S-LS	60: SILL	31: S	70: SL
Subsoil: depth (cm); texture	70: LS	100: SL	100: SL	100: LS	100: LS	100: SL
<i>Adjustments for the snowpack calculations</i>						
Snow-to-air temperature gradient multiplier	0.06	0.1	0.04	0.08	0.15	0.1
Density of fresh snow	0.15	0.15	0.12	0.16	0.3	0.12
<i>Ksat multipliers</i>						
Surface runoff	1	1	1	1	1	1
Forest floor infiltration	1	1	2	1	1	1
Forest floor interflow	2	2	0.05	1	1	2
A&B horizon infiltration	0.5	1	2	1	0.5	1
A&B horizon interflow	2	1.75	0.02	0.14	0.35	0.14
C horizon infiltration	0.5	1	2	1	0.5	1
C horizon interflow	2	2	0.05	0.5	2	2
Bedrock	Metamorphic greenschist	Granite	Sedimentary shale, sandstone	Metavolcanic Basalt	Metamorphic charnockitic gneiss	Volcaniclastic Rock: undivided Intrusive Rock
Landform	Glacial Till	Ablation Till	Ablation Till	Ablation till on basal till	Sandy Till	Colluvium
Topography	Undulating	Hummocky	Flat to rolling	Hummocky	Rolling to hummocky	Hummocky
Model Run	1999-2004	1999-2004	1994-1997	1995-2005	1990-1997	1994-2004

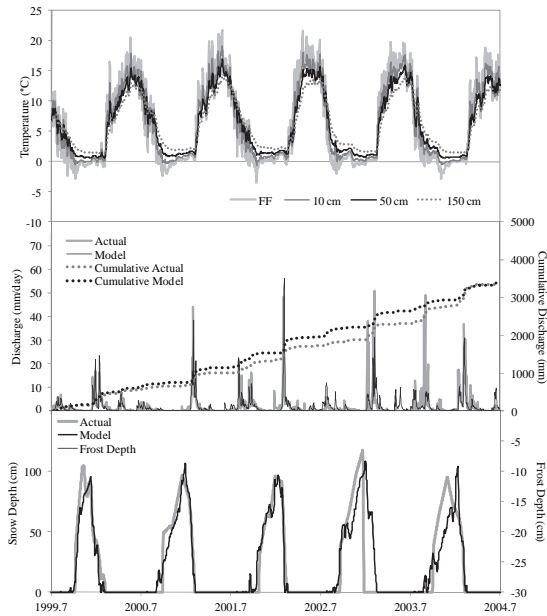
Table 3. Watershed description by site, with hydraulic conductivity adjustments.

Parameters	Moosepit Brook			Pockwock			Hayward Brook			Lac Laflamme			Turkey Lakes			Rithet River		
	FF	A&B	C	FF	A&B	C	FF	A&B	C	FF	A&B	C	FF	A&B	C	FF	A&B	C
Db, g cm ³	0.32	1.32	1.70	0.32	1.32	1.70	0.06	0.90	1.30	0.16	1.13	1.52	0.16	1.09	1.85	0.16	0.74	1.87
Dp, g cm ³	1.33	2.48	2.60	1.33	2.48	2.60	1.33	2.48	2.58	1.33	2.58	2.48	1.33	2.48	2.58	1.33	2.27	2.55
FC, %	0.28	0.21	0.15	0.28	0.21	0.15	0.27	0.10	0.12	0.13	0.12	0.05	0.27	0.18	0.16	0.30	0.26	0.17
PWP, %	0.10	0.07	0.06	0.10	0.07	0.06	0.10	0.05	0.04	0.03	0.16	0.04	0.10	0.06	0.08	0.11	0.09	0.06
Thermal conductivity, W m ⁻¹ °C ⁻¹	0.59	1.34	2.01	0.59	1.34	2.01	0.60	1.31	1.87	0.52	1.49	2.00	0.60	1.45	2.01	0.52	0.99	2.44
Heat Capacity, cal cm ⁻³ °C ⁻¹	0.42	0.46	0.57	0.42	0.46	0.57	0.35	0.36	0.48	0.46	0.35	0.43	0.49	0.47	0.56	0.41	0.44	0.54
OM, %	100	5	0.1	100	5	0.1	100	5	1	100	1	5	100	5	1	100	15	2
Coarse Fragments %	-	10	20	-	10	20	-	20	25	-	4	14	-	10	10	-	10	20
Sand, %	-	40	45	-	40	45	-	90	60	-	90	80	-	30	60	-	60	60
Clay, %	-	20	15	-	20	15	-	10	20	-	10	10	-	20	10	-	20	20
Ksat, cm hr ⁻¹ (Eq. 8)	0.30	41.50	6.65	0.30	41.50	6.65	0.30	150.00	21.70	0.30	105.60	20.53	0.30	39.80	0.10	0.30	45.67	0.58
Ksat, cm hr ⁻¹ (Eq. 8 x Table 3 multipliers)	0.30	20.75	3.33	0.30	41.50	6.65	0.60	300.00	43.40	0.30	52.80	10.27	0.30	39.80	0.10	0.30	45.67	0.58
Ksat, cm hr ⁻¹ (References)	-	-	-	-	-	-	-	-	-	-	56.63(1.8) ^a	17.07(3.1) ^a	-	-	-	-	-	-
Porosity	0.76	0.47	0.35	0.76	0.47	0.35	0.95	0.64	0.50	0.88	0.56	0.39	0.88	0.56	0.28	0.88	0.67	0.27
Porosity (References)	-	-	-	-	-	-	-	-	-	-	0.65(8.3) ^a	0.4(10.9) ^a	-	0.67 ^b	0.30 ^b	-	-	-

^a Barry et al. (1990) ^b Murray and Buttle (2005)

Table 4. Hydrothermal soil profile, needed for the daily soil moisture, temperature and stream discharge calculations (Balland et al. 2008).

Top



Bottom

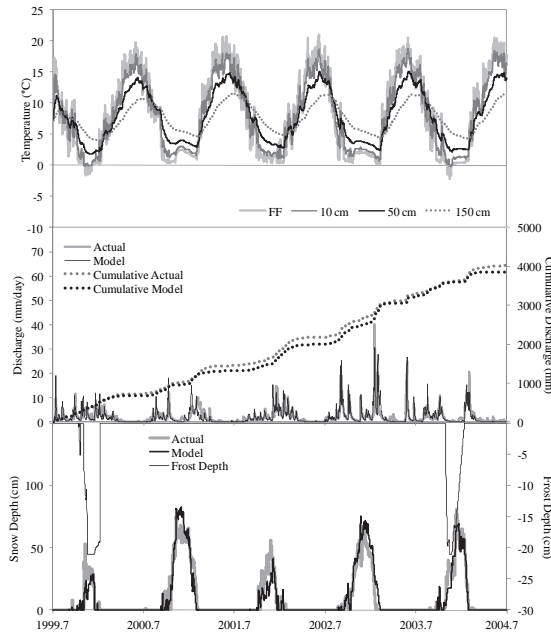


Fig. 4. ForHyM generated output for snow-on-the-ground, frost depth, soil temperature, and stream discharge (daily as well as cumulative) within the forested basins at Turkey Lakes, Ontario (top) and for the Moosepit Brook basin in Nova Scotia (bottom). Basin details: Tables 3 and 4.

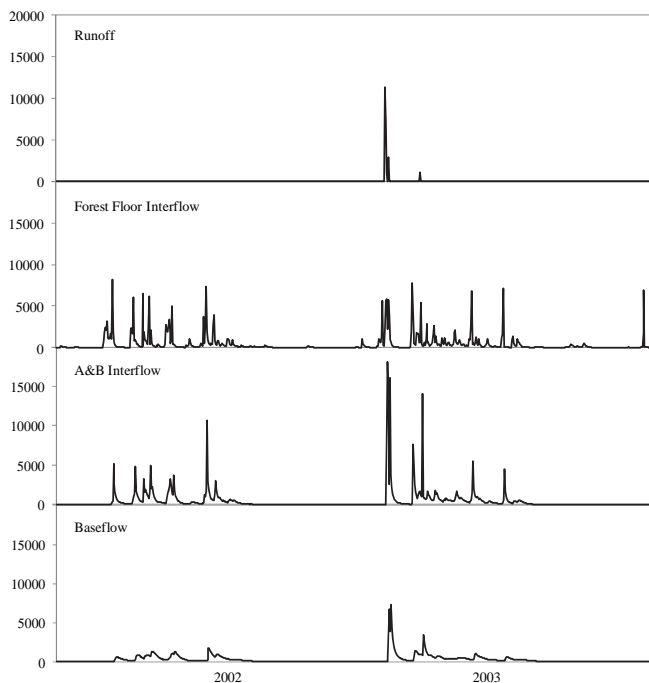


Fig. 5. ForHyM generated output for daily runoff, interflow (forest floor, A&B layers) and baseflow (in mm), for the Rithet River, BC. Basin details: Tables 3 and 4.

Site	Year		Month		Week		Day	
	R ²	β	R ²	β	R ²	β	R ²	β
Moosepit Brook	0.85	1.03	0.90	1.01	0.78	0.96	0.74	0.93
Peggy Brook	0.94	1.45	0.85	1.02	0.72	0.87	0.65	0.90
Hayward Brook	0.63	1.02	0.85	1.05	0.58	0.86	0.50	0.76
Lac Laflamme	0.81	0.95	0.55	0.85	0.55	0.74	0.48	0.67
Turkey Lakes	0.89	0.99	0.80	0.86	0.61	0.77	0.51	0.74
Rithet River	0.88	1.11	0.95	1.00	0.82	0.93	0.60	1.04

Table 5. Comparing ForHyM-modeled with measured daily, weekly, monthly and annual cumulative discharge: coefficient of determination (R²) and linear regression coefficient (β ; intercept = 0).

4. Concluding remarks

The Ksat, SP, FC, PWP values generated from layer-specific values for Db, Dp, Sand, Clay, organic matter and soil depth produce reasonable results for the extent of water retention

and flow rates for run-off, infiltration, interflow, percolation, baseflow and stream discharge across each of the six catchment areas of this study, with the layer-specific Ksat calibrations remaining within a factor of two of the generically derived Ksat estimates. For the well-drained watersheds at Turkey Lakes (Ontario), Lac Laflamme (Quebec), and Rithet River (Vancouver Island, British Columbia), however, extra downward adjustments for interflow were needed, likely due to the combined effects of (i) high slope heterogeneities, thereby leading to a slow-down of lateral flows, and (ii) the close proximity of glacially fractured bedrock beneath the regolith along ridges, thereby encouraging deep percolation instead of lateral flow. For the calcareous substrate of the Hayward Brook watershed in New Brunswick, the downward Ksat adjustments for interflow are likely due to the greater porosity of the calcareous shales, which – in turn – required upward Ksat adjustments for soil and subsoil percolation. Similar adjustments would have to be made for agricultural areas where the flow rates would be accelerated by drainage tiles and ditches. Additional Ksat adjustments would be needed where soil bulk density (Db) changes on account of surface and sub-surface compaction, weather-induced shrinking and swelling, and freezing and thawing. In conclusion, the process of:

- i. estimating Ksat, FC, PWP and soil porosity from soil survey data for soil depth, texture and organic matter,
- ii. using these estimates as initial values for modelling the daily changes in the hydrothermal conditions and flows through of forest catchments, and
- iii. subsequently calibrating Ksat to improve the run-off, infiltration, percolation, interflow and base flow calculations

generated good agreements between modelled and monitored stream discharge for the six forest catchments of this study at the daily level, year-round. The Ksat adjustments required to do so generally remained within a factor of 2 for the downward flow components. Additional adjustments were required for the catchments on steep and calcareous terrains.

5. Acknowledgements

This research was supported by the NSERC Discovery Program, by an Environment Canada grant in support of the continuing development of the Forest Hydrology Model ForHyM (c/o T. Clair), and by NSERC's Sustainable Forest Management Network on modelling and mapping hydrologically sensitive areas.

6. References

- Balland, V. 2002. Hydrogeologic watershed modelling with special focus on snow accumulation and snowmelt including retention and release of major ions. MScF thesis, University of New Brunswick, 175 p.
- Balland, V. and Arp, P.A., 2005. Modelling soil thermal conductivities over a wide range of conditions. *J. Eng. Env. Sci.* 4, 549-558.
- Balland, V, Bhatti, J. S., Errington, R., Castonguay, M., Arp, P.A., 2006. Modelling soil temperature and moisture regimes in a jack pine, black spruce and aspen forest stand in central Saskatchewan (BOREAS SSA). *Can. J. Soil Sci.* 86, 203–217.

- Balland, V., Pollacco, J. A. P. and Arp, P. A. 2008. Modeling soil hydraulic properties for a wide range of soil conditions. *Ecol. Model.* 219, 300-313.
- Barry R., Plamondon A.P., Stein J., 1987. Hydrologic soil properties and application of a soil moisture model in a balsam fir forest. *Can. J. For. Res.* 18, 427-434.
- Barry R., Prévost M., Stein J., and Plamondon A., 1990. Simulation of snowmelt runoff pathways on the Lac Laflamme watershed. *J. Hydrol.* 113: 103-121
- Beall, F. D., Semkin R. G., Jeffries D. S., 2001. Trends in the output of first-order basins at Turkey Lakes watershed, 1982-96. *Ecosystems* 4, 514-526.
- Bobba A.G., Kam D.C.L., Jeffries D.S., Bottomley D., 1986. Modelling the hydrological regimes in acidified watershed. *Water, Air and Soil Pollution.* 31, 155-163.
- Bouma, J., 1989. Using soil survey data for quantitative land evaluation. *Adv. Soil Sci.* 9, 177-213.
- Børgesen, C. D., Schaap, M.G., 2005. Point and parameter pedotransfer functions for water retention predictions for Danish soils. *Geoderma* 127, 154- 167.
- Børgesen, C. D., Iversen, B.V., Jacobsen, O.H., Schaap, M.G., 2007. Pedotransfer functions estimating soil hydraulic properties using different soil parameters. *Hydrol. Process.* DOI: 10.1002/hyp.6731.
- CANSIS, 2000. Canadian Soil Information System. Available from <http://sis.agr.gc.ca/cansis/>
- Chi X. 2008. Hydrogeological assessment of stream water in forested watersheds: temperature, dissolved oxygen, pH, and electrical conductivity. MSc thesis. University of New Brunswick, Fredericton. 161p.
- Church, M.R. 1997. Hydrochemistry of forested catchments. *Annu. Rev. Earth Planet. Sci.* 25, 23-59.
- Di Federico, V., Tartakosky, D.M., 2000. Effective hydraulic conductivity in multiscale random fields with truncated power variograms. *Geol. Soc. Am.* 348, 80-89.
- Gijssman, A., Jagtap, S.S., Jones, J. W., 2003. Wading through a swamp of complete confusion: how to choose a method for estimating soil water retention parameters for crop models. *Eur. J. Agronomy* 18, 75-105.
- Jutras, M.-F., Nasr, M., Castonguay, M., Pit, C., Pomeroy, J., Smith, T.P., Zhang, C.-F., Ritchie, C.D., Meng, F.-R., Clair, T.A., Arp, P.A. 2011. Dissolved organic carbon concentrations and fluxes in forest catchments and streams: DOC-3 model. *Ecol. Model.* in print.
- Kim, K.W., Chung, I.M., Won, Y.S., Arnold, J.G. 2008. Development and application of the integrated SWAT-MODFLOW model. *J. Hydrol.* 356, 1-16.
- Kuchment, L.S., Demidov, V.N., Startseva, Z.P. 2006. Coupled modelling of the hydrological and carbon cycles in the soil-vegetation-atmosphere system. *J. Hydrol.* 323, 4-21.
- Laudon, H., Sjöblom, V., Buffam, I., Seibert, J., Morth, M. 2007. The role of catchment scale and landscape characteristics for runoff generation of boreal streams. *J. Hydrol.* 344, 198- 209.
- Leij, F.J., Alves, W.J., van Genuchten, M.Th., Williams, J.R., 1996. The UNSODA Unsaturated Soil Hydraulic Database; User's Manual, Version 1.0. EPA/600/R-96/095, National Risk Management Laboratory, Office of Research and Development, U.S. Environmental Protection Agency, Cincinnati, OH.
<http://www.ussl.ars.usda.gov/models/unsoda.HTM>

- Murphy P.N.C., Castonguay M., Ogilvie J., Nasr M., Hazlett P., Bhatti J., Arp P.A., 2009. A geospatial and temporal framework for modelling gaseous N and other N losses from forest soils and basins, with application to the Turkey Lakes watershed project, in Ontario Canada. *For. Ecol. Management* 258, 2304-2317.
- Murray, C.D., Buttle. J.M. 2005. Infiltration and soil water mixing on forested and harvested slopes during spring snowmelt, Turkey Lakes Watershed, central Ontario. *J. Hydrol.* 306, 1-20.
- Nemes, A., Schaap, M. Wösten, H., 2003. Functional evaluation of pedotransfer functions derived from different scales of data collection. *Soil Sci. Soc. Am. J.* 67, 1093-1102.
- Pachepsky, Y., Rawls, W.L. 2005. Development of pedotransfer functions in soil hydrology. *Developments in Soil Science*, Vol. 30. Elsevier Science. 542 p.
- Paquet, J.M., Caron, J., Banton, O., 1993. In-situ determination of the water desorption characteristics of peat substrates. *Canadian J. Soil Sci.* 73, 329-339.
- Pepin, S., Plamondon, A., Stein, J., 1992. Peat water content measurement using time domain reflectometry. *Canadian J. Forest Res.* 22, 534-540.
- Schaap, M.G., 2006. Models for indirect estimation of soil hydraulic properties. *Encyclopedia of Hydrological Sciences*. DOI: 10.1002/0470848944.hsa078
- Schulze-Makuch D., Carlson D., Cherkauer D., Malik P., 1999. Scale dependency of hydraulic conductivity in heterogenous media. *Ground Water* 37, 904-919.
- Sudicky, E.A., Illman, W.A. Goltz, I.K., Adams, J.J., McLaren, R.G. 2010. Heterogeneity in hydraulic conductivity and its role on the macroscale transport of a solute plume: From measurements to a practical application of stochastic flow and transport theory. *Water Resources Research*, 46, W01508, pp. 16; doi:10.1029/2008WR007558
- Stein J., Proulx S., Lévesque D., 1994. Forest floor frost dynamics during spring snowmelt in a boreal forested basin. *Water Resources Research* 4, 995-1007.
- Vega-Nieva, D. J., Castonguay, M., Ogilvie, J., Arp, P. A., 2009. Development of a modular terrain model to estimate daily variations in machine-specific forest soil trafficability, year-round. *Can. J. Soil Sci.* 89, 93-109.
- Zhang, Y., Gable, C.W., Person, M. 2006. Equivalent hydraulic conductivity of an experimental stratigraphy: Implications for basin-scale flow simulations. *Water Resources Research*, 42, W05404, pp. 19; doi:10.1029/2005WR004720